CHALMERS

Review of research on strengthened concrete structures subjected to impulse and blast loading

RASMUS REMPLING, JOOSEF LEPPÄNEN, MARIO PLOS

Department of Civil and Environmental Engineering
Division of Structural Engineering
Concrete Structures
CHALMERS UNIVERSITY OF TECHNOLOGY
Göteborg, Sweden 2014
Report 2014:7

Report 2014:7

Review of research on strengthened concrete structures subjected to impulse and blast loading

RASMUS REMPLING, JOOSEF LEPPÄNEN, MARIO PLOS

Department of Civil and Environmental Engineering
Division of Structural Engineering
Concrete Structures
Chalmers University of Technology
Göteborg, Sweden 2014

Review of research on strengthened concrete structures subjected to impulse loading

RASMUS REMPLING, JOOSEF LEPPÄNEN, MARIO PLOS

Department of Civil and Environmental Engineering
Division of Structural Engineering
Concrete Structures
Chalmers University of Technology
SE-412 96 Göteborg
Sweden
Telephone: + 46 (0)31-772 1000

Chalmers reproservice, Göteborg, Sweden 2014

Review of research on strengthened concrete structures subjected to impulse loading

RASMUS REMPLING, JOOSEF LEPPÄNEN, MARIO PLOS

Department of Civil and Environmental Engineering

Division of Structural Engineering

Concrete Structures

Chalmers University of Technology

Abstract

It is of growing interest to innovate the structural design of fortifications, not only in military context, but also in civil applications. There is ongoing research in Sweden on concrete structures subjected to impact loading. The research done at universities is mostly directed to normal concrete and numerical studies. However, as the building materials develop and the area of applications steer towards strengthening of existing structures, it is of interest to expand the current research to also include other types of building materials, especially steel fibre reinforced concrete and high strength concrete.

The purpose of this project was to make a summary of ongoing research of strengthening of concrete structures subjected to impact loading and its aim is to collect, analyse and summarise existing knowledge.

This research project was made as a meta-analysis. The two most common scientific databases have been searched for publication.

In the report, the material response as well as the responses of different concrete compositions are discussed, compared and evaluated.

The result shows that the current research questions on concrete subjected to blast loading involve the material response of “new” concrete compositions, such as high strength and fibre reinforced concrete. In the experiments, the common approach is either a split-Hopkinson bar or a drop-weight test.

Key words: high strength concrete, fibre reinforced concrete, impulse loading, concrete structures, strengthening

Contents

Preface

The work presented in this report has been performed in the research project: “Förstudie av förstärkning av byggnader mot impulslast” that was financed by the Swedish Fortifications Agency. Rolf Dahlenius represented the Swedish Fortifocations Agency. His fruitful comments and recommendations have been of significant value for the project results.

The project group consisted of: Professor Emeritus Kent Gylltoft, Associate Professor Mario Plos, Assistant Professor Rasmus Rempling and Ph.D. Joosef Leppänen.

1 Introduction

1.1 Background

It is of growing interest to innovate the structural design of fortifications, not only in military context, but also in civil applications. There is ongoing research in Sweden on concrete structures subjected to impact loading. The research done at universities is mostly directed to normal concrete and numerical studies. However, as the building materials develop and the area of applications steer towards strengthening of existing structures, it is of interest to expand the current research to also include other types of building materials, especially steel fibre reinforced concrete and high strength concrete.

1.2 Purpose and aim

This project purpose was to do a summary of ongoing research of strengthening of concrete structures subjected to impact loading and its aim is to collect, analyse and summarise existing knowledge. A secondary objective was to propose a further investigation that should lead to recommendations for strengthening of concrete structures subjected to impact loading.

The following questions were used as basis for collecting research results with regard to the topic:

- General questions:
  - What are the current research questions?
  - What types of loads are used in the research?
  - What is the current practice of design codes?
  - What types of concrete structures are used as applications?
  - Which strengthening techniques are researched?
    - How is the strengthening done?
    - Examples, etc.
- Material questions:
  - What is the difference between high performance and high strength concrete?
    - Material characteristics that are important.
  - What types of fibres are investigated?
  - What types of high strength concrete are investigated?
  - What is the material response of fibre reinforced concrete subjected to impulse loading?
  - What is the material response of high strength concrete subjected to impulse loading?

1.3 Method

This research project has been done as a meta-analysis. The two most common databases of scientific publications have been searched for publication. The time frame was chosen to be the default of the databases: 1978-2014 and only the title and the abstract have been searched according to the following scheme:

Database	Tags	Search term	No. of articles found

EngineeringVillage	Title	IMPULSIVE AND LOADING AND CONCRETE	4
EngineeringVillage	Title	IMPACT AND LOADING AND CONCRETE	28
EngineeringVillage	Title	SHOCK AND WAVE AND LOADING AND CONCRETE	0
Web of science	Title	impact AND loading AND concrete AND strengthening	0
Web of science	Abstract	impact AND loading AND concrete AND strengthening	50

Then, the publications have been searched for the variables of the initially chosen indicators: location of researchers, nature of study, type of concrete. However, as the work developed a second set of terms was added: year, type of structure, impact velocity and strain rate.

From these indicators a script was written to extract the variables of the indicators. In order to see patterns in the data, this script was used generate a database that could be used in order to analyse and combine the data of the variables.

1.4 Limitations

- The focus was on research of fibre reinforced concrete and high strength concrete.

2 General overview of research

2.1 Overview with regard to nature of study and location

In this section the research on fibre reinforced concrete and high strength concrete subjected to impulse loading is reviewed. The time-span that the review represents is 1978-2014. The following indicators have been used to collect and analyse the research: Year of publication, Researcher location, type of concrete researched, nature of study. These are then analysed in different sets to give an overview of the research

In Table 1 and Table 2, the overview of location of research is presented with regard to year and nature of study.

Noteworthy is that North America, USA and Canada, are standing out with highest number of publications. Though, the nature of study of the individual countries is different. Canada has focused on experimental research, while USA makes numerical studies. The publications are spread out over the time-span considered.

In Asia, China, India, and Japan do research on concrete subjected impulse loading. Except for Japan the countries do both theoretical and experimental research. However, among all the countries China is the second one to do the highest number of experimental research. With regard to time, China has most recently made publications.

In Europe, former republic of Czechoslovakia and UK have made publications within the area of numerical investigations. The publications are spread out over the studied time-span.

In Australia, there are two rather recent publications including both experimental and numerical studies.

Table 1: Overview of research on concrete subjected to impulse loading with regard to location.

	Australia	*Brasil*	*Canada*	*China*	*Czechoslovakia*	*England*	*Germany*
Sum	9	1	7	14	2	2	1
	India	*Iraq*	*Israel*	*Italy*	*Japan*	*Korea*	*Malaysia*
Sum	1	1	1	1	4	1	2
	Saudi Arabia	*Singapore*	*Sweden*	*Switzerland*	*Turkey*	*UK*	*USA*
Sum	1	2	1	1	1	4	6

Table 2: Overview of research on concrete subjected to impulse loading with regard to nature of study and location.

	experiment	numerical	analytical	material model
Australia	4	3		
Brasil		1		
Canada	7			
China	6	7		
Czechoslovakia	1	2		
England	2			
Germany		1		
India	1	1		
Israel				1
Italy				
Japan	3		2	
Korea		1		
Malayisa	3	1	1	
Switzerland	1			
Saudi Arabia	1			
Singapore	1			
Sweden		1		
Turkey	1			
UK	5	5		
USA	1	1		1

To conclude:

- Research is ongoing in nearly all regions
- There is no clear difference with regard to region and nature of study. However, specific countries do specific research. One example is Canada that only does experimental research.

2.2 Overview with regard to type of concrete studies and location.

In Table 3, the type of concrete investigated in the investigations is specified with regard to location. The following types of concrete have been identified in the publications: plain concrete of standard strength, bar reinforced concrete, steel fibre reinforced concrete, plastic fibre reinforced concrete, geomaterial (basalt) fibre reinforced concrete and high strength concrete.

Bar reinforced concrete is always used as reference in any type of investigation, but especially in experimental investigations, and therefore this makes the majority of the concrete types studied. Canada does research on nearly all types of concrete. For the other countries, it is difficult to estimate with this set of data.

Table 3: Overview of research on concrete subjected to impulse loading with regard to type of concrete studies and location.

	Plain Concrete	Reinforced concrete	Steel fibre reinforced concrete	Plastic fibre reinforcement	Geomaterial fibre reinforced concrete	High strength concrete	Glass fibre reinforced concrete	Carbon fibre reinforced concrete	SUM
Australia	2		8	1					11
Brasil		1							1
Canada	2	2	6	3		2		1	16
China		2	9	1	1	1			14
Czechoslovakia		1	1						2
England			2						2
Israel			1						1
India		1							1
Iraq			1						1
Italy			1						1
Malaysia			2						2
Saudi Arabia	1		1	1					3
Singapore			1						1
Sweden			1						1
SWITZERLAND			1						1
Turkey			1	1			1		3
Japan		1	1	1					3
UK	3								3
USA		2	4	2				1	9
SUM	8	10	41	10	1	3	1	2	

To conclude:

- Canada is doing research on nearly all types of concrete

2.3 Overview with regard to type of concrete, nature of study, and time-span.

In Figure 1, investigations of type of concrete with regard to the chosen time-span are presented. As can be seen all types were investigated during the time-span except for high strength concrete that was studied in the 80's and recently in 2014.

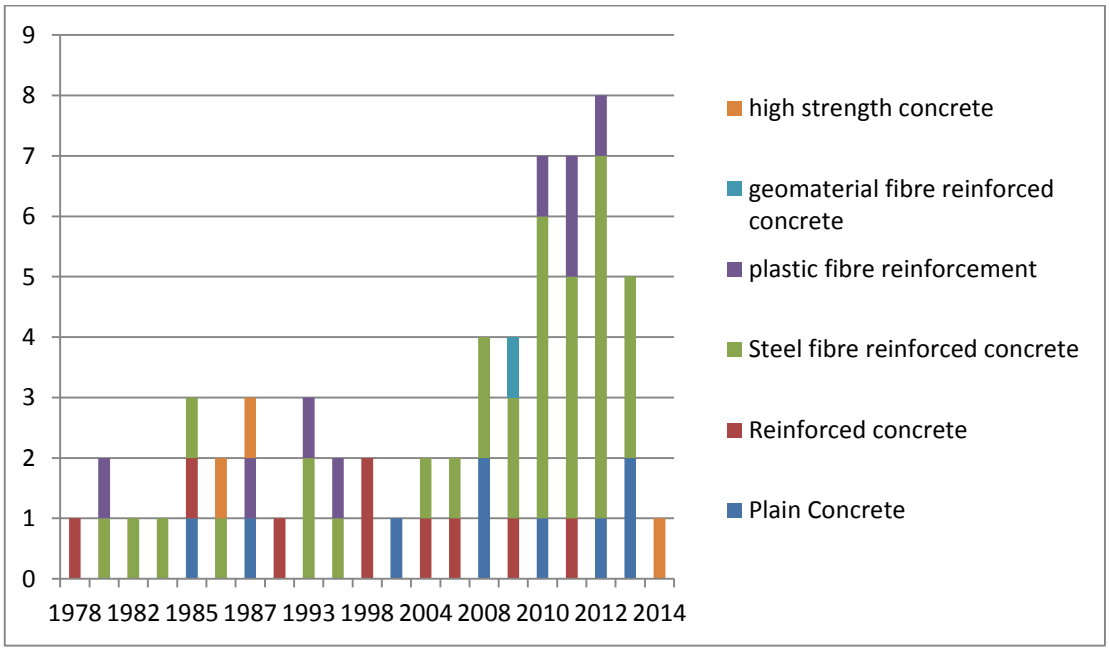

Figure 1: Overview of number of published studies on concrete subjected to impulse loading with regard to type of concrete and time-span.

In Figure 2, the nature of the study with regard to the time-span is presented. In many other areas it is noteworthy to mention that experimental investigations are becoming rare, often due to financial issues. The opposite can be seen in the area studied; experiments are still done to a large content in comparison to studies of other nature.

It also obvious that material modelling and analytical investigations are scarce, which indicates that it might be motivated with more studies of this kind.

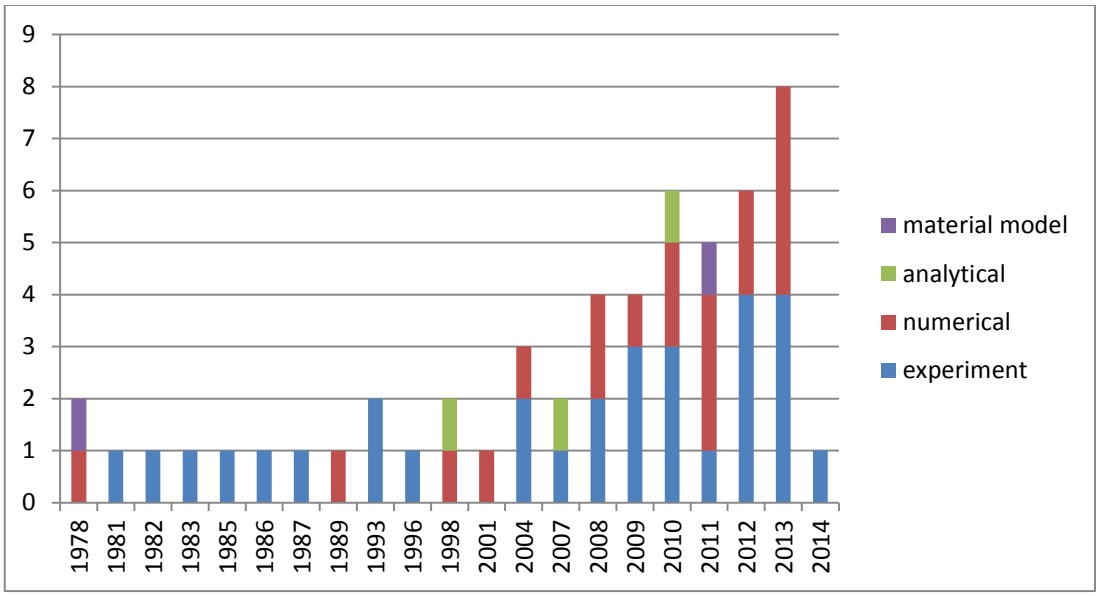

Figure 2: Overview of number of published studies on concrete subjected to impulse loading with regard to nature of study and time-span.

To conclude:

- Almost all types of concrete are included in the studies during the time-span investigated.
- Modelling and analytical investigations are scarce.

In Figure 3, the strain rates used in the investigations are presented. The focus is mainly on strain rates above 10^-2 up to 10^+2 1/s.

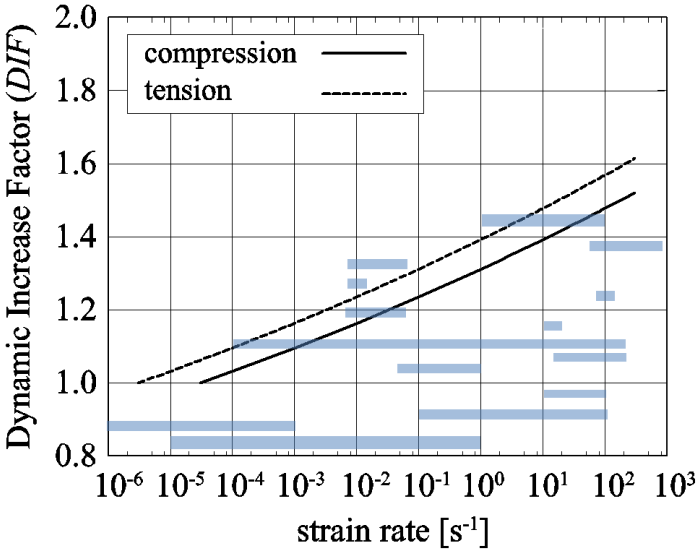

Figure 3: Overview of the strain rates used in the investigations. The reported results cover the entire area from low strain rates to very high strain rates.

3 Impulse loading

3.1 Sources of explosion load

A shock wave resulting from an explosive detonation in free air is termed an air-blast shock wave, or simply blast wave. There are different sources of explosions that cause blast wave; these can be divided in weapons, terrorist load and civil applications.

Weapons are divided in nuclear weapons and conventional weapons. Nuclear weapons are not of interest in this work and no further discussion will be presented. Conventional weapons according to Krauthammer (2000) can be divided in

a) Small arms and aircraft cannon projectiles
b) Direct and indirect fire weapon projectiles
c) Grenades
d) Bombs
e) Rockets and Missiles

Examples of small arms and aircraft cannon projectiles are pistols, rifles, machine guns or armor-piercing (AP) projectiles. Direct and indirect fire weapons projectiles belong to various types of artillery weapons; the weapons contain various amount of high explosive (HE). The weapon effects causes severe blast wave and fragmentation as well. Grenades are typical hand-delivered, but can also be launched by rifle. Grenades cause fragmentation that can severely injure or kill humans. The rifle launched grenades can penetrate approximately 500 mm concrete. Bombs are divided in HE bombs, fire and incendiary bombs, special purpose bombs and dispenser and cluster bombs.

The HE bombs can be further divided in, general-purpose (GP), light-case (LC), fragmentation (FRAG), armor piercing (AP), semi-armor piercing (SAP) and fuel-air explosive (FAE).

The explosive vary from different weapons; and produces different magnitudes of peak pressure and impulse. To establish a basis for comparison, other explosives are rated according to equivalent TNT values. According to ConWep (1992), the averaged free-air equivalent weights based on blast pressure and impulse are shown in Table 3.1.

Table 3.1 Averaged free-air equivalent weights based on blast pressure and impulse, from ConWep (1992).

Explosive	Equivalent weight pressure	Equivalent weight impulse
ANFO	0,82	0,82
Composition A-3	1,09	1,07
Composition B	1,11	0,98
Composition C-4	1,37	1,19
Cyclotol (70/130)[a]	1,14	1,09
HBX-1	1,17	1,16
HBX-3	1,14	0,97
H-6	1,38	1,15
Minol II 70/30[b]	1,20	1,11
Octol 75/25	1,06	1,06
PETN	1,27	1,27
Pentolite	1,42	1,00
	1,38	1,14
Tetryl 75/25[c]	1,07	1,07
Tetrytol 70/30	1,06	1,06
65/35	1,06	1,06
TNETB	1,36	1,10
TNT	**1,00**	**1,00**
Tritonal	1,07	0,96

a RDX/TNT
b HMX/TNT
c TETRYL/TNT

Terrorist load can be pipe bombs; bombs with different explosives in bags, cars, vans, small trucks, large trucks or trucks with trailer, see Johansson and Laine (2012).

Other sources of explosion loads are civil applications, such as tank trucks, gas canister, industries with explosive materials, e.g. refinery, chemical factories and color factory.

3.2 Blast waves

To understand the behaviour of concrete structures subjected to explosive loading, the nature and physics of explosions and the formation of a blast wave and reflections from a bomb must be understood. When the blast wave hits a concrete surface, a stress wave propagates through the concrete. An explosion is characterized by a physical or chemical change in the explosive material; this happens when there is a sudden change of stored potential energy into mechanical work, which generates a blast wave and a powerful sound, see Engberg and Karevik (1987). The explosive material can react in two ways, as a deflagration or as a detonation. For deflagration, the explosive material burns at a speed below the sonic speed, while for a detonation, the chemical reaction

occurs faster than the sonic speed. In military situations, detonations are the most common; for example, if a TNT charge explodes, this means that it decays as a detonation.

The blast environment differs according to where the explosion takes place. In an airburst, when the blast wave hits the ground surface, it is reflected. The reflected wave coalesces with the incident wave, forming a Mach front, as shown in Figure 3.1. The point at which the three shock fronts meet – incident wave, reflected wave and the Mach front – is termed the triple point.

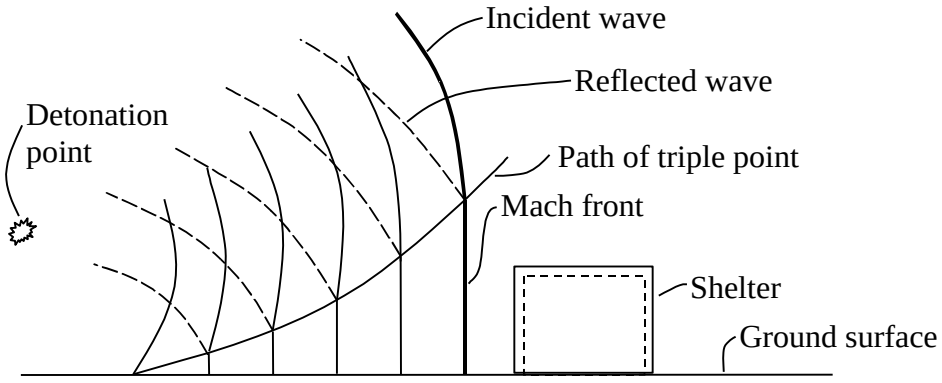

Figure 3.1 Blast environment from an airburst, based on Krauthammer (2000).

When there is a surface burst, the reflection occurs instantaneously from the ground surface, which generates a shock wave; this is termed a ground-reflected wave, as shown in Figure 3.2. At a short distance from the burst, the wave front can be approximated by a plane wave.

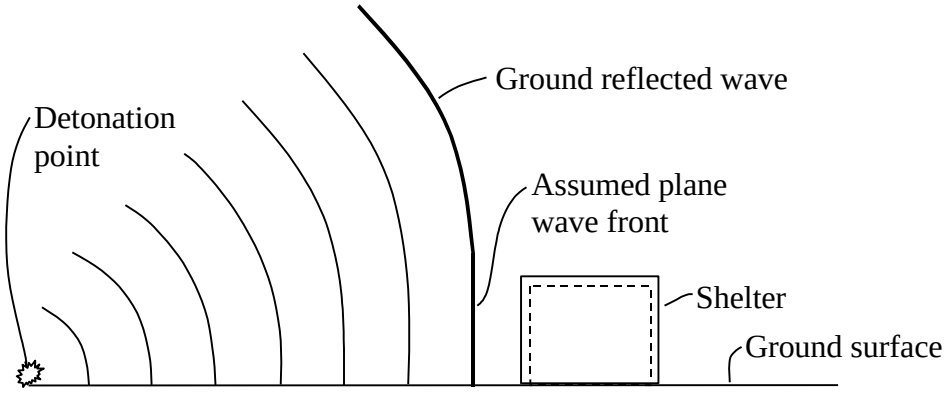

Figure 3.2 Surface burst blast environment, based on Krauthammer (2000).

The pressure–time history of a blast wave can be illustrated with a general curve as shown in Figure 3.3. The illustration is an idealization of an explosion. The pressure-time history is divided into positive and negative phases. In the positive phase, maximum overpressure, $P_0 + P_s^+$, rises instantaneously and then decays to atmospheric pressure, P_0, with time, t^+. The positive impulse, i^+, is the area under the positive phase of the pressure-time curve. For the negative phase, the maximum negative pressure, $P_0 - P_s^-$, has much lower amplitude than the maximum overpressure. The duration of the negative phase, t^-, is much longer than that of the positive one. The negative impulse, i^-, is the area below the negative phase of the pressure-time curve. The positive phase is more interesting in studies of blast wave effects on concrete buildings because of the

high amplitude of its overpressure and the concentration of the impulse.

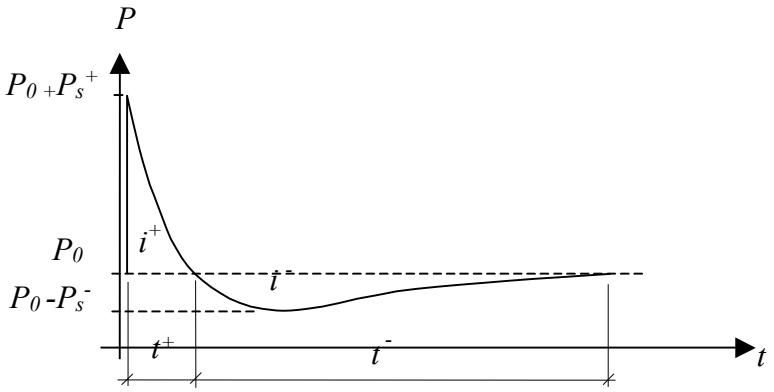

Figure 3.3 Pressure-time history from a blast.

The following exponential form expresses the pressure-time history in Figure 3.3, first noted by Friedlander (1939), according to Bulson (1997):

$$P(t) = P_0 + P_s^+(1-\frac{t}{t^+})e^{-\alpha t/t^+} \tag{3.1}$$

where $P(t)$ is the overpressure at time t and t^+ (the positive duration) is the time for the pressure to return to the atmospheric level P_0. By selecting a value for the constant α various pressure-time histories can be described. The peak pressure $P_0 + P_s^+$ depends mainly on the distance from the charge and the weight of the explosives. In addition, if the peak pressure, the positive impulse and the positive time duration are known, the constant α can be calculated, and then the pressure-time history can be obtained.

Equation (3.1) is often simplified with a triangular pressure-time curve; see Bulson (1997):

$$P(t) = P_0 + P_s^+(1-\frac{t}{t^+}) \tag{3.2}$$

The impulse can be calculated by the following equation; see Johansson (2012):

$$i^+ = P^+t^+\left(\frac{1}{\alpha}-\frac{1}{\alpha^2}(1-e^{-\alpha})\right) \tag{3.3}$$

A scaling parameter is introduced, first noted by Hopkinson (1915); see Bulson (1997). With the parameter Z it is possible to calculate the effect of a detonated explosion, conventional or nuclear, as long as the equivalent weight of charge in TNT is known:

$$Z = \frac{r}{W^{1/3}} \tag{3.4}$$

where r is the distance from the detonation and W is the equivalent weight of TNT. The peak pressure, the positive duration time and the positive impulse are now functions of Z, and the pressure-time history in Figure 3.3 can be described:

$$P_s^+(Z)$$
$$\frac{t^+}{\sqrt[3]{W}}(Z) \tag{3.5}$$
$$\frac{i^+}{\sqrt[3]{W}}(Z)$$

The peak pressure for undisturbed air blast according to FKR (2011) can be calculated as:

$$P_s^+ = 10^y \text{ [kPa]} \tag{3.6}$$

where

$$y = 2{,}6113 - 1{,}6901 \cdot \alpha + 0{,}0080497 \cdot \alpha^2 + 0{,}33674 \cdot \alpha^3 - 0{,}0051622 \cdot \alpha^4 - 0{,}080923 \cdot \alpha^5 - 0{,}0047851 \cdot \alpha^6 + 0{,}0079303 \cdot \alpha^7 + 0{,}00076845 \cdot \alpha^8 \tag{3.7}$$

and with

$$\alpha = -0{,}21436 + 1{,}3503 \cdot \log(Z) \tag{3.8}$$

equation is valid for the interval:

$$0{,}0531 < Z < 40 \tag{3.9}$$

Z according to equation (3.4).

The positive impulse for undisturbed air blast according to FKR (2011) can be calculated as:

$$i_s^+ = 10^y \cdot \frac{W^{1/3}}{1000} \text{ [kPas]} \tag{3.10}$$

where

$$y = 2{,}3883 - 0{,}44375 \cdot \alpha + 0{,}16882 \cdot \alpha^2 + 0{,}034814 \cdot \alpha^3 - 0{,}010435 \cdot \alpha^4 \tag{3.11}$$

and with

$$\alpha = 2{,}3472 + 3{,}2430 \cdot \log(Z) \tag{3.12}$$

equation is valid for the interval:

$$0{,}0531 < Z < 0{,}792 \tag{3.13}$$

Z according to equation (3.4).

For the interval:

$$0{,}792 < Z < 40 \tag{3.14}$$

the following expression is used:

$$y = 1{,}5520 - 0{,}40463 \cdot \alpha - 0{,}014272 \cdot \alpha^2 + 0{,}0091237 \cdot \alpha^3 - 0{,}00067507 \cdot \alpha^4 - 0{,}0080086 \cdot \alpha^5 + 0{,}0031482 \cdot \alpha^6 + 0{,}0015204 \cdot \alpha^7 - 0{,}00074703 \cdot \alpha^8 \tag{3.15}$$

and with

$$\alpha = -1{,}7531 + 2{,}3063 \cdot \log(Z) \tag{3.16}$$

Z according to equation (3.4).

The positive duration time, valid for undisturbed air blast and reflected blast waves (see section 3.3) as well, according to FKR (2011) can be calculated as:

$$t^{+} = 10^{y} \cdot W^{1/3} \,[\text{ms}] \tag{3.17}$$

where

$$\begin{aligned} y = {} & -0{,}6866 + 0{,}16495 \cdot \alpha + 0{,}12779 \cdot \alpha^2 + 0{,}0029143 \cdot \alpha^3 + 0{,}0018796 \cdot \alpha^4 \\ & + 0{,}017341 \cdot \alpha^5 + 0{,}002697 \cdot \alpha^6 - 0{,}0036198 \cdot \alpha^7 - 0{,}0010093 \cdot \alpha^8 \end{aligned} \tag{3.18}$$

and with

$$\alpha = 2{,}2637 + 5{,}1159 \cdot \log(Z) \tag{3.19}$$

equation is valid for the interval:

$$0{,}147 < Z < 0{,}888 \tag{3.20}$$

Z according to equation (3.4).

For the interval:

$$0{,}888 < Z < 2{,}28 \tag{3.21}$$

the following expression is used:

$$\begin{aligned} y = {} & 0{,}23031 - 0{,}29794 \cdot \alpha + 0{,}30633 \cdot \alpha^2 + 0{,}018341 \cdot \alpha^3 - 0{,}017396 \cdot \alpha^4 \\ & - 0{,}0010632 \cdot \alpha^5 + 0{,}0056206 \cdot \alpha^6 + 0{,}00016822 \cdot \alpha^7 - 0{,}00068602 \cdot \alpha^8 \end{aligned} \tag{3.22}$$

and with

$$\alpha = -1{,}3336 + 9{,}2996 \cdot \log(Z) \tag{3.23}$$

Z according to equation (3.4).

For the interval:

$$2{,}88 < Z < 40 \tag{3.24}$$

the following expression is used:

$$\begin{aligned} y = {} & 0{,}62104 + 0{,}096703 \cdot \alpha - 0{,}008013 \cdot \alpha^2 + 0{,}0048271 \cdot \alpha^3 \\ & + 0{,}0018759 \cdot \alpha^4 - 0{,}0024674 \cdot \alpha^5 - 0{,}00084112 \cdot \alpha^6 + 0{,}00061933 \cdot \alpha^7 \end{aligned} \tag{3.25}$$

and with

$$\alpha = -3{,}1301 + 3{,}1525 \cdot \log(Z) \tag{3.26}$$

Z according to equation (3.4).

3.3 Blast wave reflections

When a blast wave strikes a surface which is not parallel to its direction of propagation, a reflection of the blast wave is generated. The reflection can be either normal or oblique. There are two types of oblique reflection, either regular or Mach; the type of reflection depends on the incident angle and shock strength.

3.3.1 Normal reflection

A normal reflection takes place when the blast wave strikes perpendicular to a surface, as shown in Figure 3.4. The medium (normally air) has a particle velocity U_x before the incident shock wave U_s passes through the medium; after passage the particle velocity increases to U_p. Furthermore, the overpressure increases from P_x to P_y (P_x usually refers to atmospheric overpressure), the temperature rises from θ_x to θ_y and the sonic speed rises from c_x to c_y (c_x is approximately 340 m/s in undisturbed air).

When the blast wave hits a rigid surface, the direction is abruptly shifted, and, as a consequence, the particles at the surface possess a velocity relative to those further from the surface: this relative velocity is equal in magnitude and reversed in direction from the original particle velocity. This has the effect of a new shock front moving back through the air: the reflected shock U_r. However, since the air conditions have changed, the reflected shock does not have the same properties. The reflected overpressure increases to P_r, temperature rises to θ_r and sonic speed is c_r.

For shock waves it is common to describe the velocity as a Mach number, which is defined as the actual velocity (of the shock front) in the medium, divided by the sonic speed of the undisturbed medium. For example, the shock front has a velocity, with a Mach number, M_r, through air that had a velocity of M_x when the incident shock occurred, as shown in Figure 3.4.

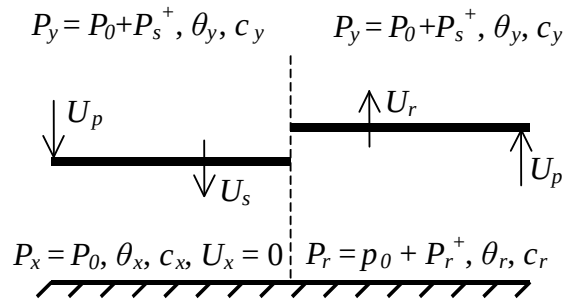

Figure 3.4 Normal reflection in air from a rigid wall, based on Baker (1973).

The properties of the reflected blast wave can be described in terms of a reflection coefficient, defined as the ratio of reflected overpressure to the overpressure in the incident blast wave. It can be shown that for an ideal gas, with a specific gas constant ratio of 1,4, the reflection coefficient Λ is, according to Baker (1973),

$$\Lambda = \frac{P_r - P_x}{P_y - P_x} = \frac{8M_x^{\,2} + 4}{M_x^{\,2} + 5}. \tag{3.27}$$

From equation (3.27) it can be seen that for a shock front moving with M_x equal to one, i.e. at sonic speed, the reflection coefficient is two. This means that the overpressure is doubled in the reflected blast wave. As the speed of the shock front M_x rises, the reflection coefficient approaches eight. However, this applies to ideal gas with a specific gas constant ratio of 1,4. In a real blast wave, the specific gas constant ratio is not constant, and the coefficient is pressure-dependent, see Johansson (2012). The reflection coefficient rises with increasing pressure.

The reflected pressure for a blast wave according to FKR (2011) can be approximately

being estimated as:

$$P_r^+ \approx 2 \cdot P_s^+ \left(\frac{4P_s^+ + 7P_0}{P_s^+ + 7P_0} \right) \tag{3.28}$$

Alternatively, the peak pressure for a reflected air blast according to FKR (2011) can be calculated as:

$$P_r^+ = 10^y \text{ [kPa]} \tag{3.29}$$

where

$$\begin{aligned} y &= 3{,}2295 - 2{,}2140 \cdot \alpha + 0{,}035119 \cdot \alpha^2 + 0{,}6576 \cdot \alpha^3 \\ &+ 0{,}014181 \cdot \alpha^4 - 0{,}24308 \cdot \alpha^5 - 0{,}015870 \cdot \alpha^6 \\ &+ 0{,}049274 \cdot \alpha^7 + 0{,}0022764 \cdot \alpha^8 - 0{,}0039713 \cdot \alpha^9 \end{aligned} \tag{3.30}$$

and with

$$\alpha = -0{,}21436 + 1{,}3503 \cdot \log(Z) \tag{3.31}$$

equation is valid for the interval:

$$0{,}0531 < Z < 40 \tag{3.32}$$

Z according to equation (3.4).

The positive impulse for a reflected air blast according to FKR (2011) can be calculated as:

$$i_r^+ = 10^y \cdot \frac{W^{1/3}}{1000} \text{ [kPas]} \tag{3.33}$$

where

$$y = 2{,}5588 - 0{,}90312 \cdot \alpha + 0{,}10177 \cdot \alpha^2 - 0{,}024214 \cdot \alpha^3 \tag{3.34}$$

and with

$$\alpha = -0{,}20400 + 1{,}3788 \cdot \log(Z) \tag{3.35}$$

equation is valid for the interval:

$$0{,}0531 < Z < 40 \tag{3.36}$$

Z according to equation (3.4).

3.3.2 Regular reflection

In a regular reflection, the blast wave has an incident shock at M_x with an angle of β, and reflection takes place. The reflected shock at M_r has an angle of δ as shown in Figure 3.5. The angle of reflection is not usually equal to the angle of incidence. The air conditions in front of the incident shock (Region 1) are still at pressure P_x and temperature θ_x. Behind the incident shock (Region 2), the air is the same as for open-air shock, with pressure P_y and temperature θ_y. The air conditions from the reflected shock (Region 3), have pressure P_r and temperature θ_r.

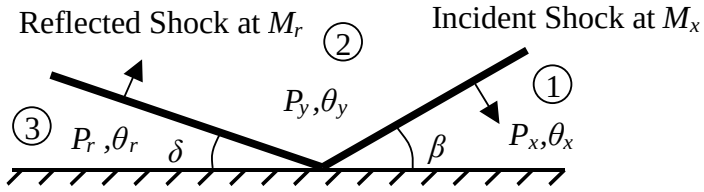

Figure 3.5 Oblique reflection, based on Baker (1973).

3.3.3 Mach stem formation

There is a critical angle, related to the shock strength, at which there cannot be an oblique reflection. According to Baker (1973), Ernst Mach [Mach and Sommer (1877)] showed that the incident shock and the reflected shock coalesce to form a third shock front. This third shock front, termed the Mach stem or Mach front, moves approximately parallel to the ground surface, as shown in Figure 3.6, as the shock front rises. The point at which the three shock fronts meet is termed the triple point. The Mach front and the path of the triple point are also shown in Figure 3.1.

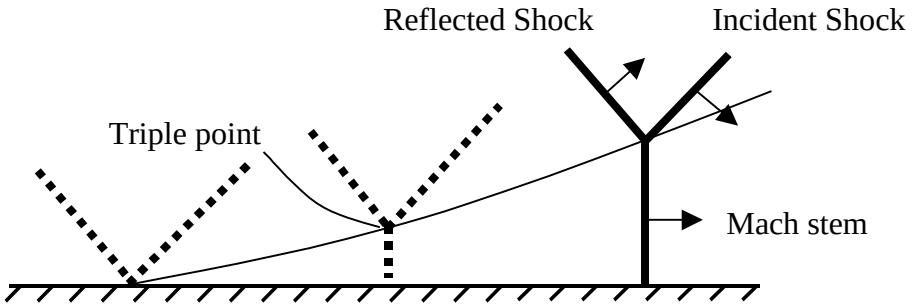

Figure 3.6 Mach stem formation, based on Baker (1973). The arrows indicate the directions of the shock waves.

4 Level of focus and type of structure.

It is interesting to derive the level of focus and the type of structure that the investigations deal with. From Tabel 1, it is seen that there is an even distribution between studies on material level and studies on different kinds of structures. Among the structures, the panel types (slabs/walls and plates) are most common.

It is also notable that the interest moves from studies of the material response to include more and more plates at a first, but later also slabs and walls.

Tabel 1: Distribution of the level of focus and the type of structures that the studies include.

Year	Beam	Block	Barriers	Slabs/Walls	Plate	Material level
1981						1
1982						1
1983						1
1985	1					
1986	1					
1987	1					
1989					1	
1993					1	1
1996	1					
1998					1	1
2001						1
2004					1	1
2007				2	1	
2008					1	1
2009		1		1		2
2010	2		1	1		1
2011				4		1
2012						6
2013				3		1
SUM	6	1	1	11	6	19

5 Methodologies for assessing fibre reinforced concrete

In this chapter, different structural assessment and material response methodologies are presented. First, a methodology that considers a wave propagation in the material is presented and secondly, a methodology that assess the response at impact.

A common methodology to test the dynamic stress-strain response of materials is the Split-Hopkinson pressure bar, named after Bertram Hopkinson. It measures the stress pulse propagation in a specimen and by using two of these bars (split bars) in series the stress-strain can be evaluated. There are several modifications, but the main idea is the same for all types. The specimen is placed between the ends of two straight bars, called the incident bar and the transmission bar. At the end of the incident bar (some distance away from the specimen, typically at the far end), a stress wave is created which propagates through the bar toward the specimen. This wave is the incident wave. The incident wave splits into two smaller waves when it reaches the specimen: one travels through the specimen and into the transmitted bar, causing deformation in the specimen. The other wave, called the reflected wave, is reflected away from the specimen and travels back down the incident bar. In Figure 4 and Figure 5, two different set-ups are presented: one for medium strain rates and one for high strain rates.

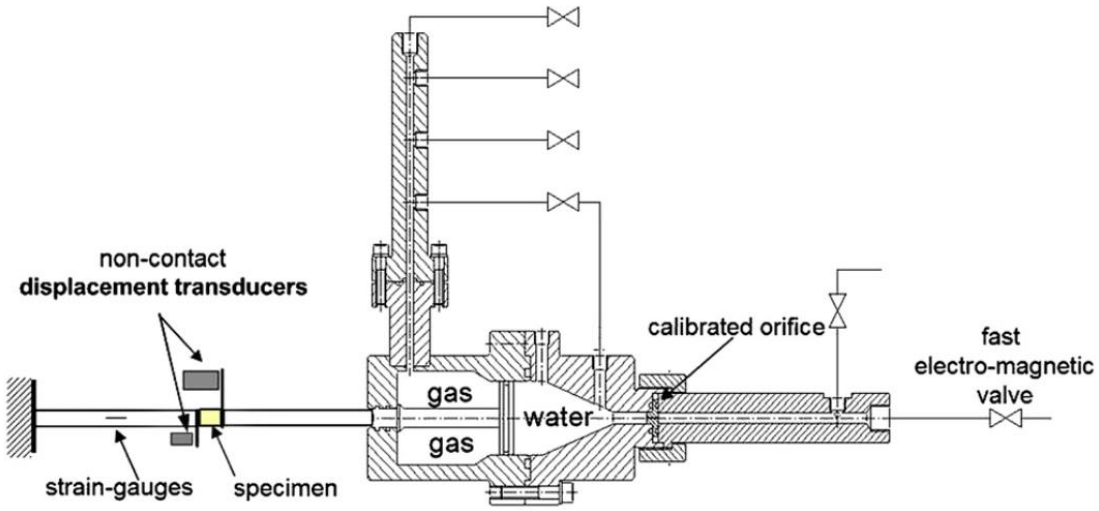

Figure 4: (Caverzan et al. 2012) Used a Hydro-pneumatic machine to investigate the material response at medium strain rates.

Figure 5: (Caverzan et al. 2012) used a Modified Hopkinson bar in order to investigate the material response at high strain rates.

In order to assess the impact response of concrete a common approach is to use a drop weight set-up. In Figure 6 and Figure 7, two examples are presented. The drop weight test descends from testing the temperature limit of welds, i.e. at which temperature the failure change from ductile to brittle. The test uses a hammer that is dropped from a specific height on the specimen, normally a beam. An accelerometer at the bottom of the specimen is used to assess the dynamic action.

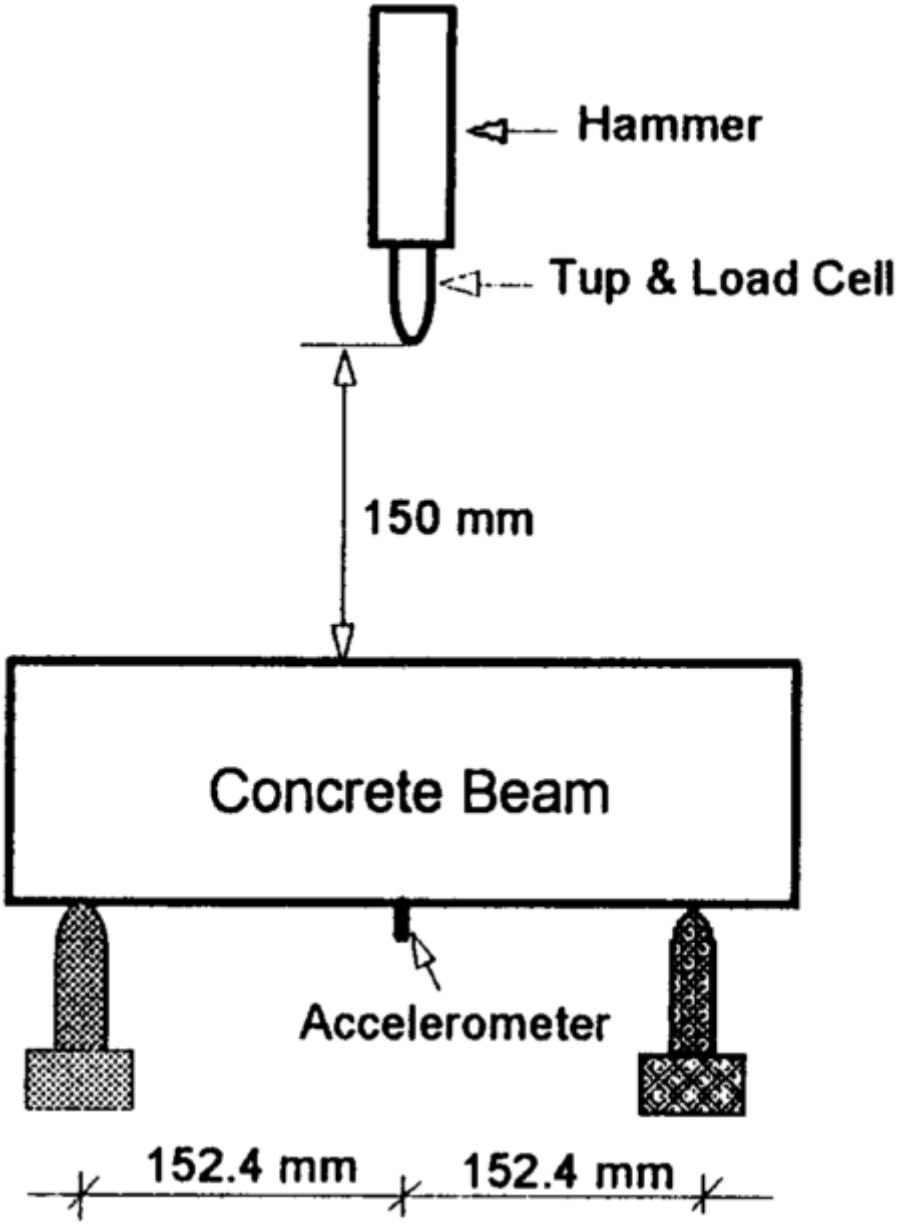

Figure 6: Impact test on concrete beam used by (Wang et al. 1996).

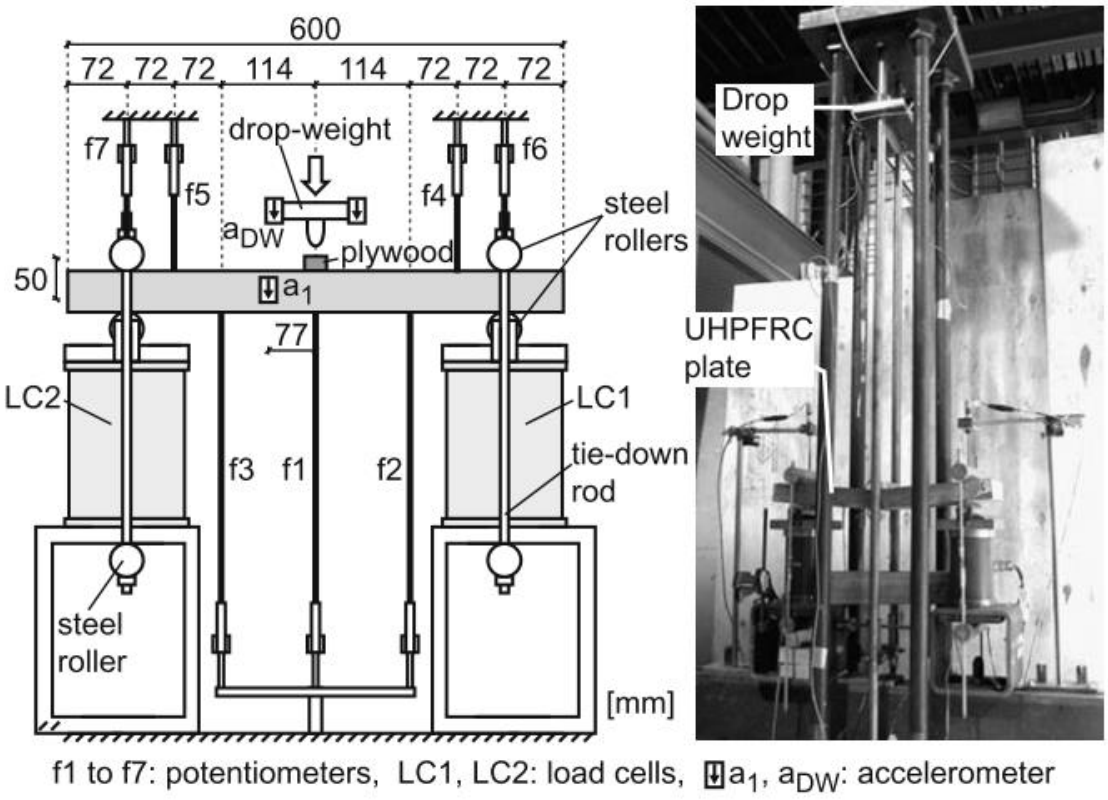

Figure 7: (Habel & Gauvreau 2008) used this set-up for drop-weight tests on fibre reinforced beams.

6 Material and structural response

6.1 High strength concrete subjected to static- and fatigue loading

Within the last two decades, the development and application of high-strength concrete has greatly increased all over the world. High-strength concrete is no longer only applied to offshore concrete structures and bridges, but also to high-rise buildings and prefabricated elements, etc. Concrete is a highly heterogeneous material because of its composite structure, which on a meso-level is a mixture of cement paste, water, air voids, and aggregates in a range of sizes and shapes. (Neville & Aïtcin 1998) found that the modulus of elasticity of the aggregate and the hardened cement paste, or rather the difference between them, strongly influences the mechanical behaviour of concrete. In HSC, there is a smaller difference between the modulus of elasticity of the hardened cement paste and that of the aggregates. The higher degree of homogeneity of a high-strength concrete results in less crack formation than in a lower-strength concrete. For instance, this results in the more linear pre-peak stress-strain behaviour and the increased compressive strength. However, close to the maximum compressive strength, larger macro-cracks are created; the subsequent failure can be sudden or even explosive. In HSC the cracks regularly pass through the aggregates, which consume less energy than when the cracks are forced to go around them as in NSC. Hence, concrete becomes more and more brittle as the compressive strength increases.

The classical empirical experiments on fatigue are the so called Wöhler tests. These load-controlled tests define the fatigue strength of a material on a macroscopic level. The fatigue strength of a material is defined as the maximum stress which the material can sustain for a given number of cycles. State of the arts reports on fatigue of normal concrete may be found in (CEB 1988) and ACI committee 215 (ACI - 215). However, similar investigations are scarce on high-strength concrete. This lack of knowledge is mentioned in CEB/FIP Bulletins 197 and 228 as well as in the report of the national research council (Zia et al. 1997). The conclusions of these reports are contradicting. The CEB/FIB Bulletin 197 concludes that the fatigue strength is comparable with static strength, while CEB/FIP Bulletin 228 says that such assumption is unnecessarily conservative. In addition, a third hypothesis is added by (Kim & Kim 1999) that had observed increased fatigue crack propagation with increased concrete quality. (CEB-FIP 2008) on high strength concrete comments on the effect of the moisture condition, which is more pronounced, on the fatigue strength. The report conclude that dried specimen showed a higher fatigue resistance, (Petkovic 1991) support this conclusion.

Investigations on the mechanisms involved are very scarce. (Mucha 2003) describes crack growth observed with high solution light microscopy system and relates the fatigue propagation to micro-cracking. However, (CEB-FIP 2008) concludes that “the controlling structural mechanisms of the fatigue behaviour have not been clarifies to an acceptable conclusion”.

6.2 Fiber reinforced concrete subjected to static- and fatigue loading

By dispersing fibers in concrete it is possible to increase the ductility and enhance the response. The fibers limit the development of macro-cracks and make it possible to transfer large stresses in the softening response. The fatigue of fiber reinforced concrete

has been investigated at the Department of Structural Engineering, Chalmers, by (Hanjari 2006), who did splitting test of both normal concrete and fiber reinforced concrete. In the literature (Grzybowski & Meyer 1993), (Paskova & Meyer 1997) and (Lee & Barr 2004), all have conflicting conclusions of which fiber content is optimal and if there exists an upper limit of fiber content where there is no benefit.

The mechanisms involved in fatigue of fiber reinforced concrete are believed to be related to the dual effect that the fibers introduce. Introducing fibers in concrete increases the pore density and thus the initial micro-cracks which could be a starting point for fatigue crack propagation. On the other hand, the fibers bridge the micro-cracked zones which lead to a more ductile response. However, these hypotheses need more investigations.

6.3 High strength concrete subjected to blast loading

There is only limited information about the response of high strength concrete subjected to impulse loading. This regards both structural response and the response on the material level. Two papers from the reviewed literature have been selected to describe this response: (Li et al. 2011) that made a numerical analysis of steel fibre-reinforced high-strength concrete walls and (Wang et al. 2012) who performed Split Hopkinson tests on fibre-reinforced high-strength concrete.

With the rapid development of computer technology and numerical techniques more accurate results can be expected from numerical modelling. In addition, as experiments that involve blast loading are expensive, numerical techniques is an interesting approach to study the response of high strength concrete subjected to blast loading. (Li et al. 2011) performed a numerical assessment of steel fibre-reinforced high-strength concrete walls of a size of 3m*3m and a thickness of 0.2m. The modelled concrete was assumed to have a compressive strength of 105MPa. They used solid elements in the model of the fully fixed wall. With this approach, they studied the response by scaling the distance between a reference point on the wall and the centre of the explosion with the mass of the explosives. This scaling gives essentially different shapes of the blast wave's front; where a smaller number is closer to a shock wave. In Figure 8, the main result of their study is presented. The figure shows that the deformation of the wall increases with a shock wave. It is also interesting to notice that for the largest distance, Z=1.5, the wall reflects the wave, i.e. the reference point experience negative displacement. According to the paper, this shows that the wall is experiencing an elastic response that can be contributed to the material type. Experimental results of the simulated wall have been reported in Chinese only. Therefore, these results have not been included in this report.

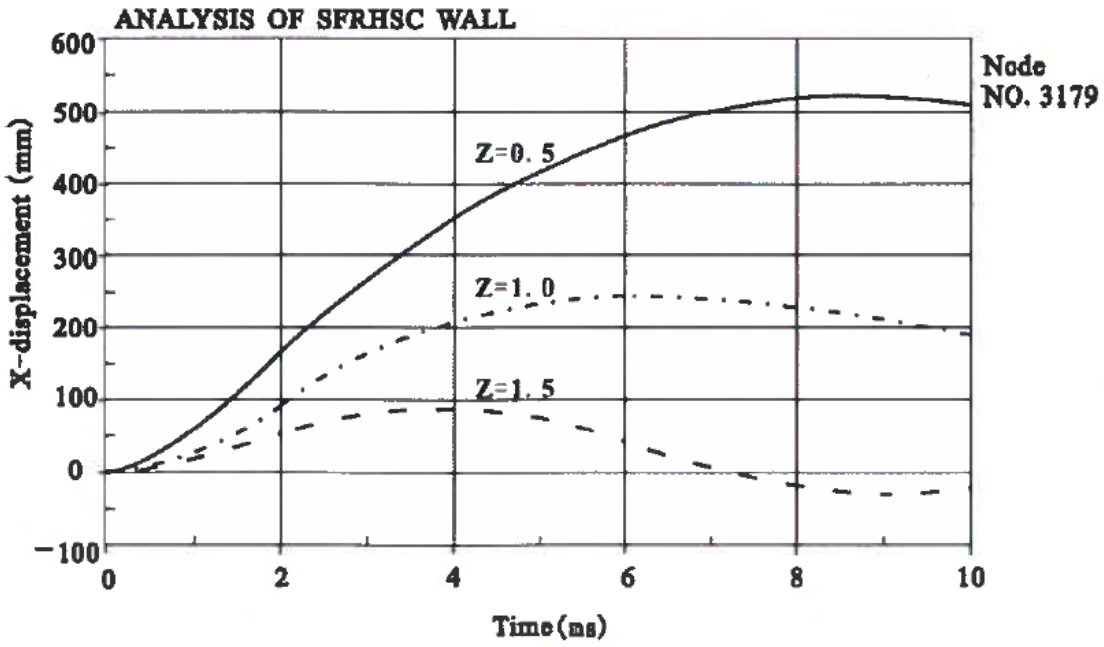

Figure 8: The displacement of the reference point on the analysed wall for different scaled distances between the explosion and the wall. Z=0.5 is supposed to simulate a blast shock wave.

Although a structure may show structural elasticity during a numerical test, it does not reveal information about the mechanical behaviour of the material. (Wang et al. 2012) have tried to contribute to this understanding by performing an experimental investigation by the means of a Split Hopkinson bar. The tested concrete has a compressive strength between 80 and 90MPa. The applied strain rate varies between 4*10^+1 and 3*10^+2. They studied the fracture patterns of the specimens, concrete matrix, and fibers. In Figure 9, the stress-strain response is presented for strain rates ranging around 10^+2 and 2.7*10^+2. It is clear that the stress-strain response of high-strength concrete is brittle and the fibre reinforced concrete types are ductile. There is no significant difference in the stress-strain response between the fibre reinforced concrete types. However, when examining the post-peak results it is revealed that a higher loading rate seems to result in a more ductile material behaviour.

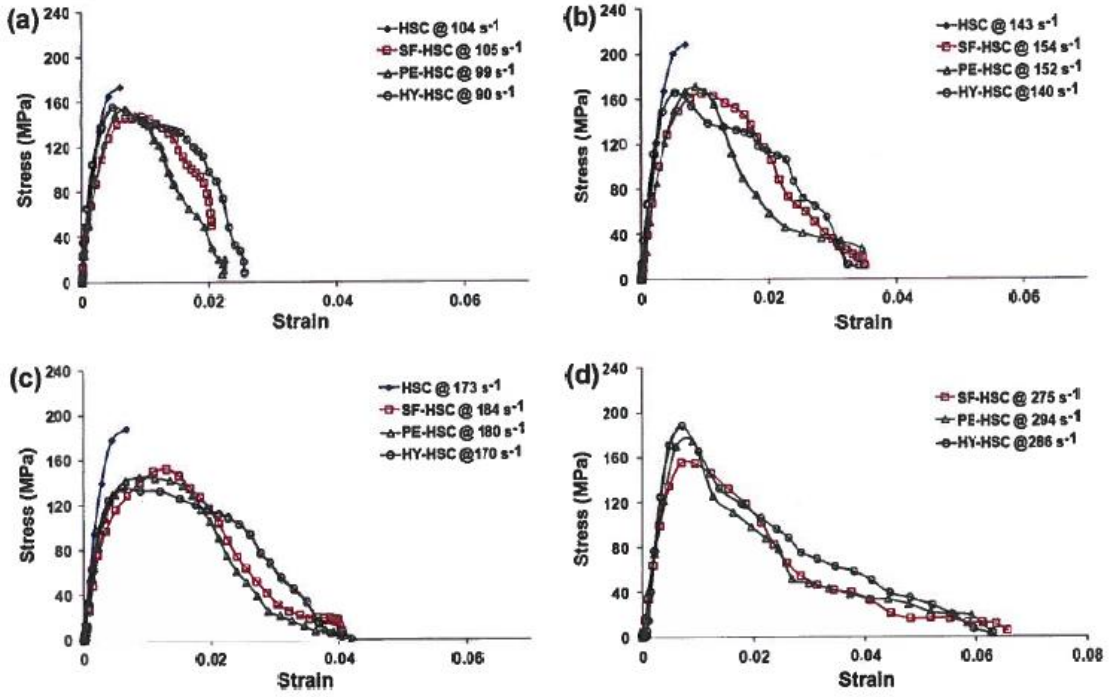

Figure 9: Results from (Wang et al. 2012) of experiments on high-strength concrete (HSC), steel-fibre reinforced high-strength concrete, polyethylene-fibre reinforced high-strength concrete, and a 50/50 combination of steel and polyethylene-fibre reinforced high-strength concrete.

6.4 Fiber reinforced concrete subjected to blast loading

(Daniel 2002) gives a comprehensive review of different fibers used for reinforcing concrete subjected to blast loading. Essentially, they are: steel fibers, glass fibers, synthetic fibers and natural fibers.

There are numerous investigation performed on fibre reinforced concrete subjected to blast loading ranging from material test to large contact detonation tests and numerical analysis of structural response and material behaviour: (Li et al. 2011; Coughlin et al. 2010; Wang et al. 2008; Fang & Zhang 2013; Almusallam et al. 2013; Nam et al. 2011; Haido et al. 2010; Lok et al. 2004; Wang et al. 2009; Banthia et al. 1993; Xu et al. 2012b; Gokoz & Naaman 1981; Xu et al. 2012a; Wang, L. P. Wu, et al. 2010; Millard et al. 2010; Tabatabaei et al. 2013; Ohtsu et al. 2007; Naaman & Gopalaratnam 1983; Foglar & Kovar 2013; Gal & Kryvoruk 2011; Wang et al. 2012; Daniel 2002; Yamaguchi et al. 2011; Wang, J. Wu, et al. 2010). Some of these papers have been reviewed more carefully and the reviews are presented below.

6.4.1 Numerical assessment

(Wang, J. Wu, et al. 2010) was interested in studying the crater size from a projectile hitting a plate structure of 60mm. The structure was modelled to represent concrete of 95-105 MPa compression resistance and the structure was reinforced with steel fibers of different ratio. The projectile hit the structure with a velocity of 1500 m/s. In Figure 10, the contour plots of the analysis is shown. The conclusion of the study is that the higher amount of steel fibers results in a higher energy absorption and, thus, a smaller penetration of the projectile.

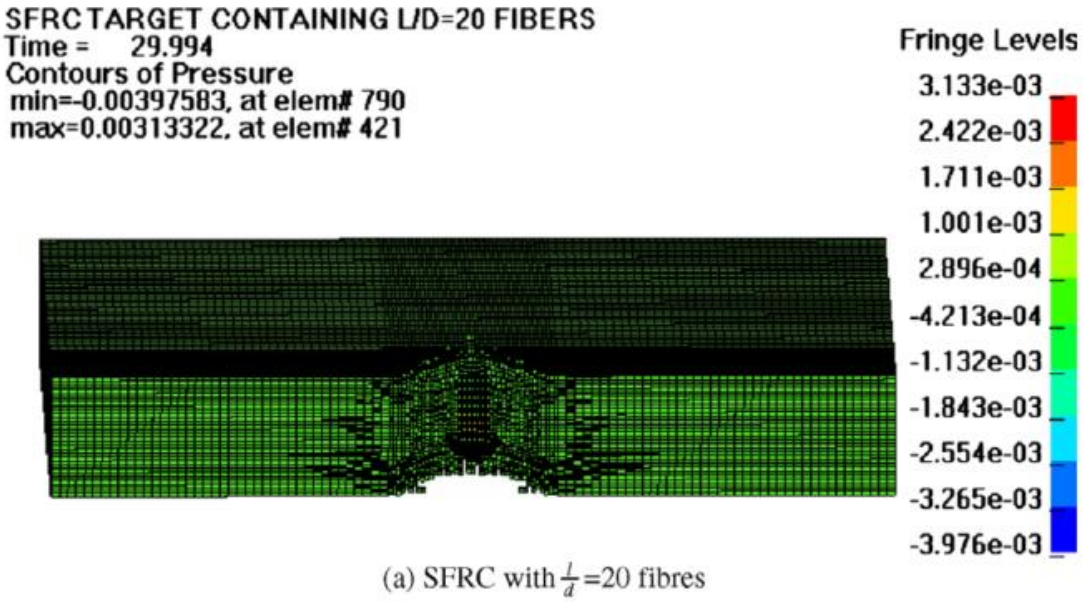

(a) SFRC with $\frac{l}{d}$=20 fibres

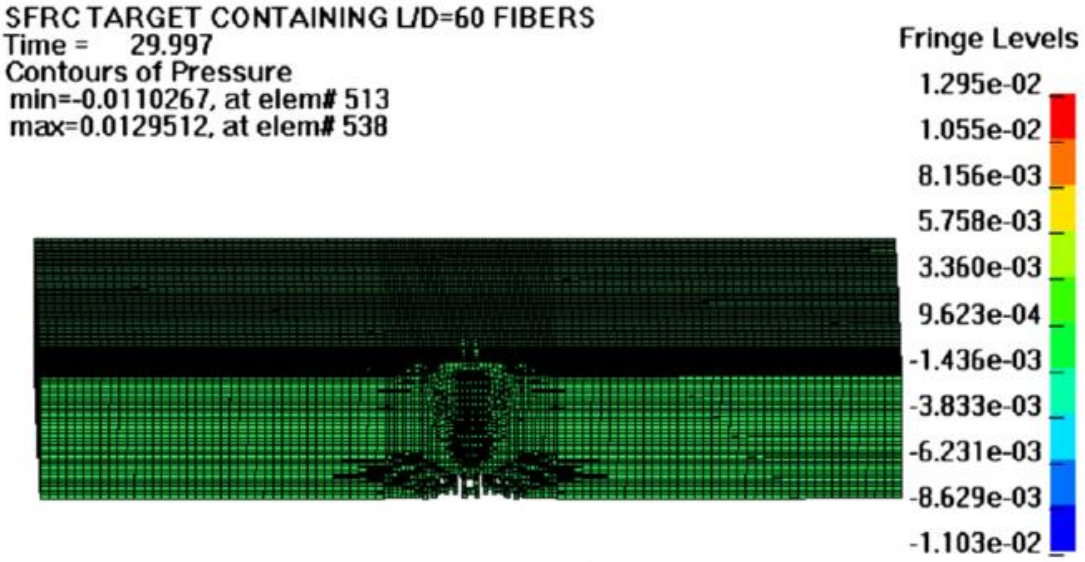

(b) SFRC with $\frac{l}{d}$=60 fibres

Figure 10: The contour plots show modelling results from (Wang, J. Wu, et al. 2010) on steel-fibre reinforced concrete. Two different ratios of steel-fibers were analysed: L/D=20 and 50 fibers.

6.4.2 Split-Hopkinson bar

(Caverzan et al. 2012) performed experimental research by means of a Modified Hopkinson bar. The investigation aimed at studying four strain rates: (10^-1, 10^0, 1.5*10^+2 and 3.0*10^+2 1/s) and the tests results were compared with the static behaviour. The tested steel-fibre reinforced concrete had a volume fraction of fibers equal to 1.25%. They used two different test machines: hydro-pneumatic machine (HPM) was used for the intermediate strain rates and a Modified Hopkinson bar (MHB) was used for the high strain rates. Comparison between static and dynamic tests highlighted several relevant aspects. The average of the stress versus crack opening displacement curves and fracture energy versus crack opening displacement is plotted

in Figure 11. The main evidence found for the increased contribution of steel fibers to the performance is the increase in strength and fracture energy. In Figure 11 C, it is worth observing the increasing initial stiffness with the increase of strain rates. This increase is much more evident when the strain rate is equal to 1.5*10^+2 or 3.0*10^+2. The initial plateau seen in the same Figure is representative for the contribution of steel fibers.

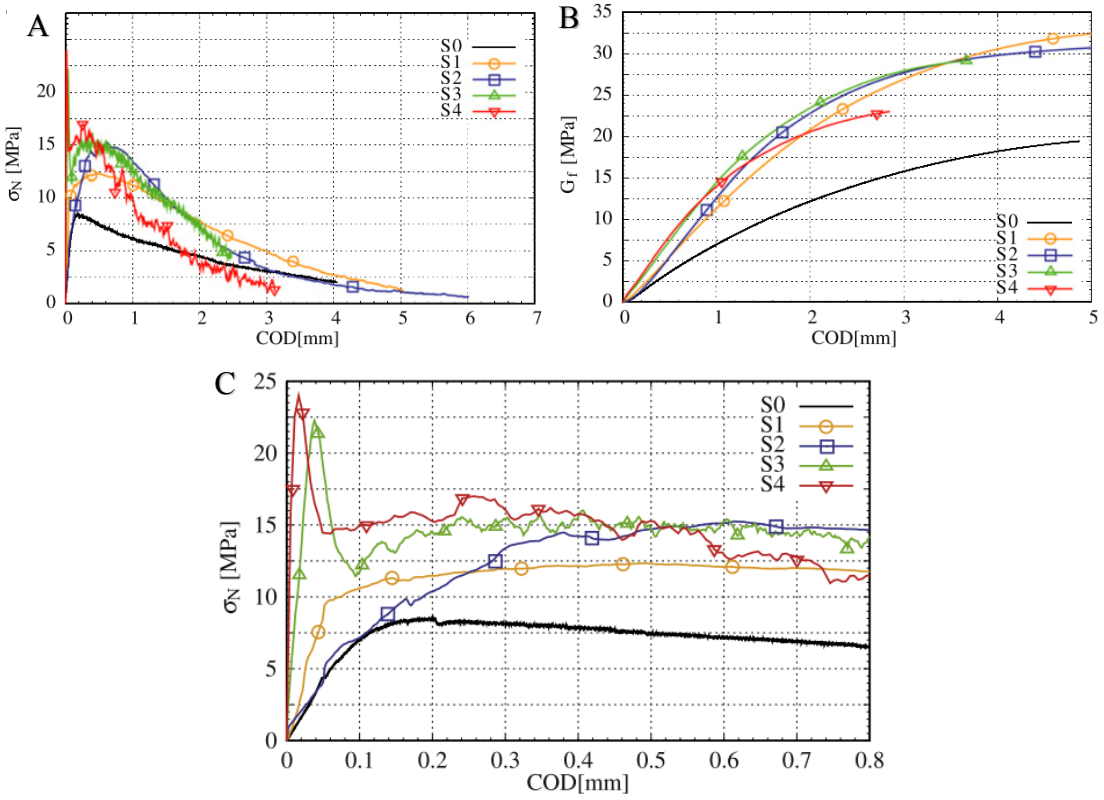

*Figure 11: This figures presents experimental results (modified Hopkinson bar) from (Caverzan et al. 2012) of steel-fibre reinforced concrete. The diagrams show: A, the average of the stress versus crack opening displacement curves; B, fracture energy versus crack opening displacement; C, detail of the peak zone. For different strain rates: S0=quasi static strain rate, S1=10^-1, S2=10^+0, S3=1.5*10^+2, and S4=3.0*10^+2.*

6.4.3 Drop-weight impact system

(Xu et al. 2012b) performed experimental investigations using two 180 t fast response load cells, a high-speed video camera in a drop-weight impact system. The investigations included several fibre types with different shapes and material properties: synthetic fibres, undulated, cold rolled, flattened, hooked end, and two new spiral shape steel fibres developed in this study. A volume fraction of 1% fibre was used in all specimens. The concrete matrix for all FRC specimens was mixed to obtain a compressive strength of 35MPa. Two different strain rates was tested simply by raising the drop-weight to different heights. The clues searched for were: axial inertia effects and the stress wave propagation effect, as well as the failure process, displacement and velocity responses of specimens, which are used to estimate the strain and strain rates of the specimen under impact loading. Strain gages were also used for direct strain measurements.

In Figure 12, the results are shown. The results demonstrate that the new spiral steel fibre proposed in this study provides better confinement to concrete matrix and thus better bonding to concrete material, therefore increases the dynamic resistance and energy absorption capacity (toughness) of FRC. On the other hand, there is only a small difference between the plain specimen and the fibre reinforced specimens.

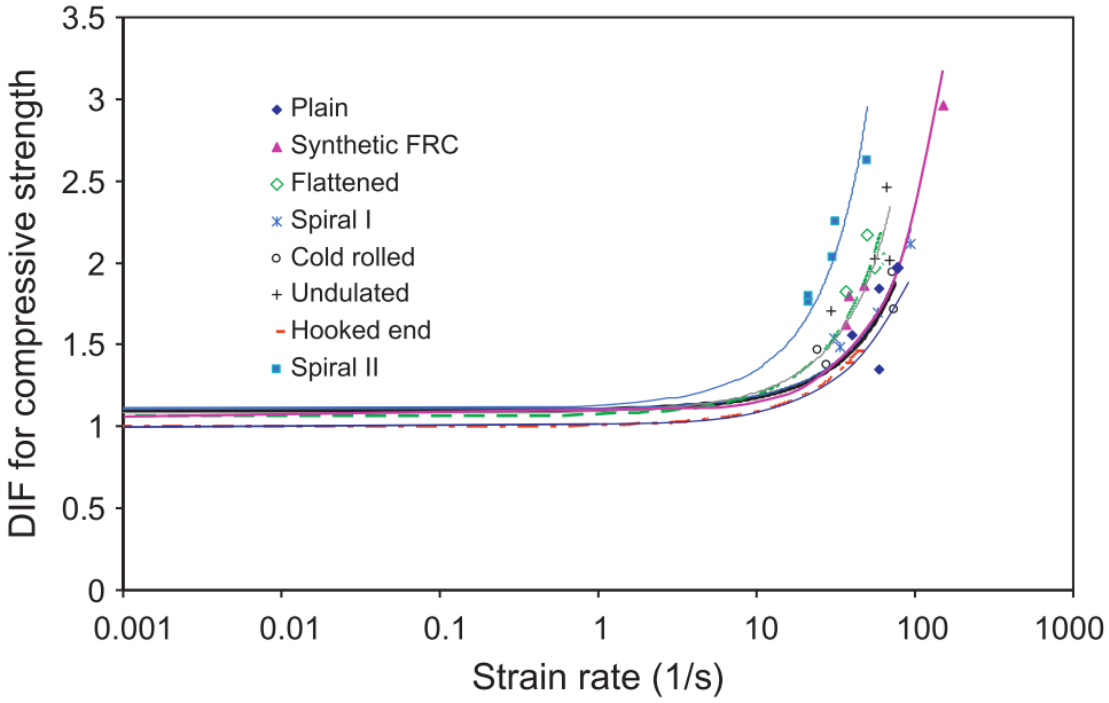

Figure 12: Dynamic increase factor for different fiber types presented in (Xu et al. 2012b).

(Mindess et al. 1987) studied the fracture toughness of plain concrete, high strength concrete, and concrete reinforced with fibrillated polypropylene fibers. A set-up of single-edge notched beams, of dimensions 1400xl00x125 mm, were loaded dynamically in 3-point bending, using an instrumented drop weight impact machine. The beams were loaded using three different drop heights of the impact hammer. It was found that the fracture toughness values under impact loading were much higher than those obtained in static tests. There were also dramatic increases in the fracture energies under impact loading. Figure 13, shows energy absorbed up to the peak load, and total fracture energy, as a function of hammer drop height. Two things that are in evidence are the unchanged absorbed energy before peak-load has been reached, and, though small, but still significant increase of absorbed energy after peak-load for the polypropylene fiber reinforced specimen. Notable is also the decrease of absorbed energy for the specimen of high-strength concrete.

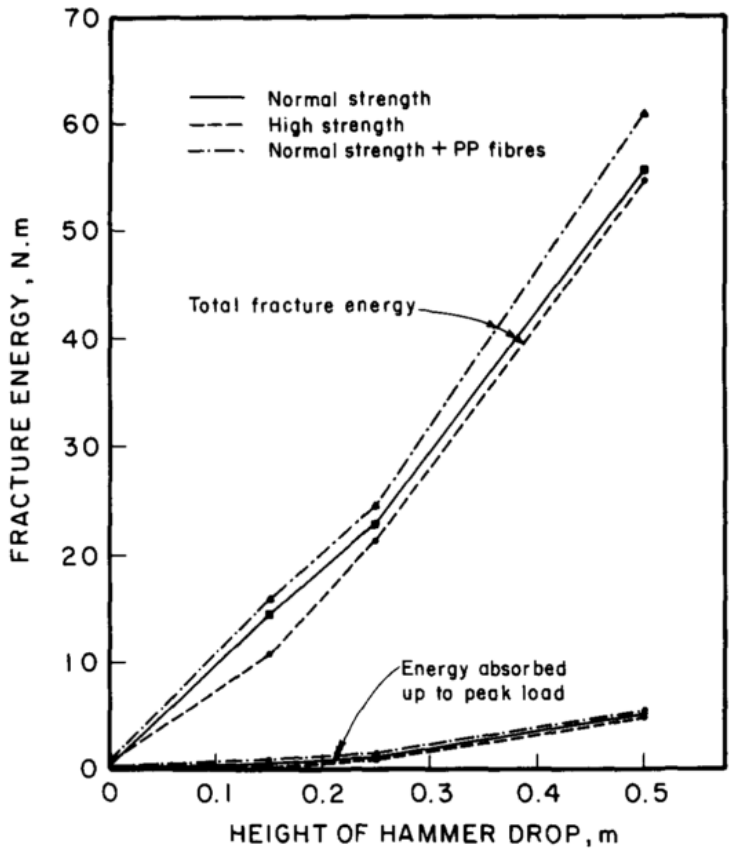

Figure 13: Test results from (Mindess et al. 1987) showing energy absorbed up to the peak load, and total fracture energy, as a function of hammer drop height.

(Habel & Gauvreau 2008) performed drop-weight tests in order to apply dynamic three-point-bending loading to steel-fibre reinforced concrete plates. The test series consisted of 26 plate specimens made of mortar like concrete reinforced with a large amount of steel fibers (Volume fraction of 5.5%). The concrete compressive strength were measured to 131MPa. Each plate had a length of 600 mm, a width of 145mm and a depth of 50 mm. Two different weights were used: 10.3 kg and 20.6 kg. The speed at impact was estimated to 4.2 m/s for the 10.3 kg weight and 4.3 m/s for the 20.6 kg weight. The testing developed no cracks on the upper surface of the specimens. This was investigated by visual inspections after each drop. All specimens showed very fine multiple cracks in the central portion of the lower surface, which are typically observed for strain hardening materials. The final fracture of the specimen occurred by fiber pullout in one localized crack which exhibited a very rough fracture surface. The failure mode for all specimens was in bending.

6.4.4 Impact test for assessing the structural behaviour

(Wang et al. 1996) performed impact tests on small concrete beams (0.10x0.10x0.35)m. The beams were reinforced with different volumes of both polypropylene and steel fibres. Nine beams were tested in total. It was found that, at volume fractions less than 0.5%, polypropylene fibres gave only a modest increase in fracture energy. Steel fibres could bring about much greater increases in fracture energy, with a transition in failure modes occurring between steel fibre volumes of 0.5% and 0.75%. Below 0.5%, fibre breaking was the primary failure mechanism and the increase in fracture energy was also modest; above 0.75% fibre pull-out was the primary mechanism with a large increase in fracture energy. In Figure 14, the fracture energy for the tested beams is

displayed.

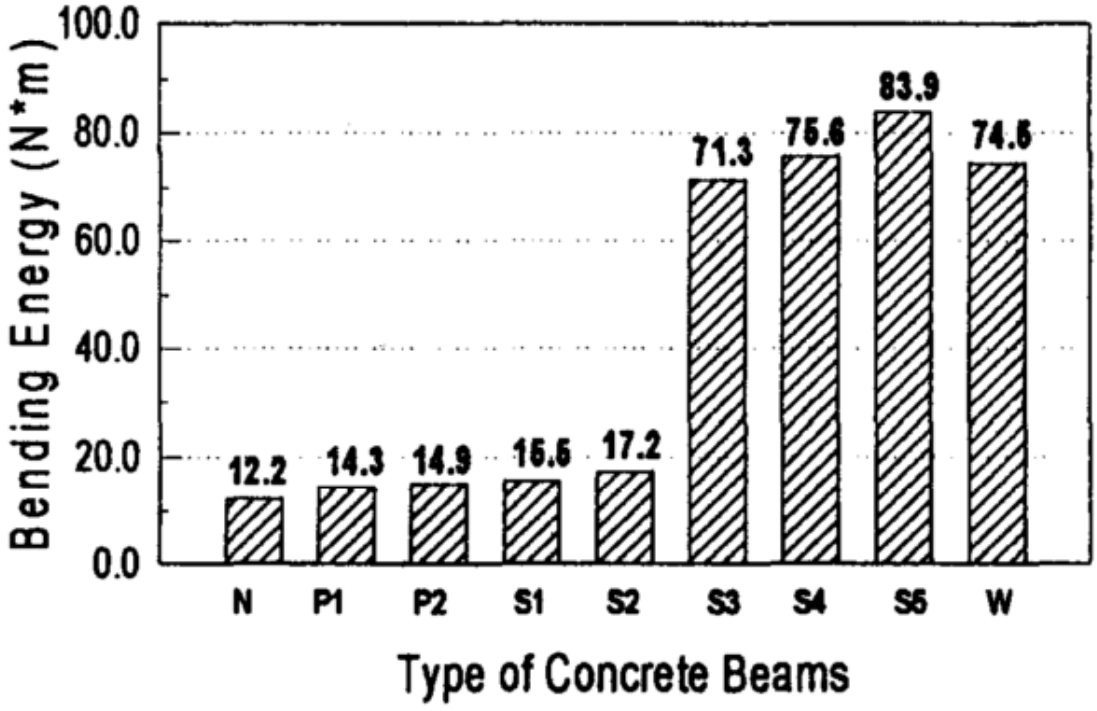

Figure 14: Bending (Fracture) energy for beams reinforced with different fibers: N=No fibers, P1=0.25% polypropylene-fibers, P2=0.50% polypropylene-fibers, S1=0.25% hooked steel-fibers, S2=0.50% hooked steel-fibers, S3=0.75% hooked steel-fibers, S4=1.00% hooked steel-fibers, S5=1.50% hooked steel-fibers, and w=0.75% crimped steel-fibers.

7 Discussion

The material responses of high strength concrete and fibre reinforced concrete subjected to blast loading are not yet defined. The number of reported studies is scarce. From the few studies made it is possible to see trends that response of high-strength concrete is more brittle than the response of the fibre reinforced concrete. Ductile means, in this context, a higher fracture energy due to a larger tail of the post-peak stress-strain response. Interesting is though, that research has shown that higher strain rates result in a more ductile material behaviour. Researchers have not given any explanation to this yet and there exists a need for more qualitative studies on the internal material mechanism.

It was thought that the study should reveal the applicability of the materials in structural applications, but the type of studies found on structural response focus on the global material behaviour and not on the structural appliances of the material. However, there exist results that show a potential of using both high-strength and fibre reinforced concrete, but no study singles out a recommendation of optimal material composition for structures subjected to blast loading.

The methods involved are traditional when it comes to investigate the material response of structures. However, recent studies involve more numerical analyses, which is natural as the computer power increases rapidly. The number of investigations will probably continue to increase due to the unsure international situations. Moreover, most probably the investigations will follow the same trend: study of new material compositions by numerical methods. In order to add to this research, it is important to continue the development and assessment of the existing numerical methods. On strive in particular, is to understand the limitations of the available numerical methods. If there is an interest to branch this trend, an analytical study of how to add a new composition to an existing in order to strengthen the existing structure is motivated.

8 Conclusion

The current research questions on concrete subjected to blast loading involve the material response of "new" concrete compositions, such as high strength and fibre reinforced concrete. In the experiments, the common approach is either a split-Hopkinson bar or a drop-weight test.

There are no studies on strengthening techniques or adding a new composition to an existing in order to strengthen the existing.

The main difference between high strength concrete and fibre reinforced concrete is that the high strength concrete has a more brittle response.

Several different types of fibres are studied but there is no significant difference in response between the types

The reviewed studies do not reveal any internal mechanisms that are significant for the response of blast loads.

8.1 Further research

The following areas have been identified for further studies:

- Investigate current practise of strengthening of concrete structures subjected to impulse loading in Sweden, by studying performed strengthening projects and mapping of problem and solution.
- An analytical study of how to add a new composition to an existing in order to strengthen the existing structure.
- A survey of the applicability of current standards on the strengthening of existing structures.
- The assessment of standards and codes in practice is lacking in the reported research. Such studies are of most importance, in order to assess their applicability. Therefore, it is proposed to make a study in which the codes of current practice are assessed by use of the experimental investigations found in this study.

9 Acknowledgement

This project was financed by the Swedish Fortifications Agency represented by Rolf Dahlenius.

10 References

Not yet written

Almusallam, T.H. et al., 2013. Response of hybrid-fiber reinforced concrete slabs to hard projectile impact. *International Journal of Impact Engineering*, 58, pp.17–30.

Banthia, N. et al., 1993. Fiber-Reinforced Cement Based Composites Under Tensile Impact. *Advanced Cement Based Materials*, 1(1), pp.131–141.

Caverzan, A., Cadoni, E. & di Prisco, M., 2012. Tensile behaviour of high performance fibre-reinforced cementitious composites at high strain rates. *International Journal of Impact Engineering*, 45, pp.28–38.

CEB, 1988. *Fatigue of concrete structures, State of the art report*,

Coughlin, a. M. et al., 2010. Behavior of portable fiber reinforced concrete vehicle barriers subject to blasts from contact charges. *International Journal of Impact Engineering*, 37(5), pp.521–529.

Daniel, J.I. (ACI C. 544), 2002. *ACI 544.1R-96 State-of-the-Art Report on Fiber Reinforced Concrete*,

Fang, Q. & Zhang, J., 2013. Three-dimensional modelling of steel fiber reinforced concrete material under intense dynamic loading. *Construction and Building Materials*, 44, pp.118–132.

Foglar, M. & Kovar, M., 2013. Conclusions from experimental testing of blast resistance of FRC and RC bridge decks. *International Journal of Impact Engineering*, 59, pp.18–28.

Gal, E. & Kryvoruk, R., 2011. Meso-scale analysis of FRC using a two-step homogenization approach. *Computers & Structures*, 89(11-12), pp.921–929.

Gokoz, U.N. & Naaman, E., 1981. Effect of strain-rate on the pull-out behaviour of fibres in mortar. *International Journal of Cement Composites and Lightweight Concrete*, 3(3).

Grzybowski, M. & Meyer, C., 1993. Damage accumulation in concrete with and without fiber reinforcement. *ACI Mater J*, 90(6), pp.594–604.

Habel, K. & Gauvreau, P., 2008. Response of ultra-high performance fiber reinforced concrete (UHPFRC) to impact and static loading. *Cement and Concrete Composites*, 30(10), pp.938–946. Available at: http://linkinghub.elsevier.com/retrieve/pii/S0958946508001133 [Accessed November 13, 2013].

Haido, J.H., H, A.B.B. & Jayaprakash, J., 2010. Nonlinear Response of Steel-Fiber Reinforced Concrete Beams under Blast Loading : Material Modeling and

Simulation. In *Advances in FRP Composites in Civil Engineering*. pp. 27–30.

Hanjari, K.Z., 2006. *Evaluation of WST Method as a Fatigue Test for Plain and Fiber-reinforced Concrete - experimental and numerical investigation*. Chalmers University of Technology.

Kim, J.-K. & Kim, Y.-Y., 1999. Fatigue crack growth of high-strength concrete in wedge-splitting test. *Cement and Concrete Research*, 29(5), pp.705–712. Available at: http://www.sciencedirect.com/science/article/pii/S0008884699000253 [Accessed April 1, 2014].

Lee, M.K. & Barr, B.I.G., 2004. An overview of the fatigue behaviour of plain and fibre reinforced concrete. *Cement and Concrete Composites*, 26(4), pp.299–305. Available at: http://apps.webofknowledge.com/full_record.do?product=WOS&search_mode=Refine&qid=15&SID=R2PZY5yriesOzVS1e5a&page=1&doc=2 [Accessed March 24, 2014].

Li, N. et al., 2011. Numerical Analysis of Steel Fiber Reinforced High Strength Concrete Walls Subjected to Blasting Load. *Applied Mechanics and Materials*, 94-96, pp.57–62.

Lok, T.S., Asce, M. & Zhao, P.J., 2004. Impact Response of Steel Fiber-Reinforced Concrete Using a Split Hopkinson Pressure Bar. , (February), pp.54–59.

Millard, S.G. et al., 2010. Dynamic enhancement of blast-resistant ultra high performance fibre-reinforced concrete under flexural and shear loading. *International Journal of Impact Engineering*, 37(4), pp.405–413.

Mindess, S. (University of B.C., Banthia, N. (University of B.C. & Yan, C. (University of B.C., 1987. The fracture toughness of concrete under impact loading. *Cement and Concrete Research*, 17, pp.231–241.

Naaman, a. E. & Gopalaratnam, V.S., 1983. Impact properties of steel fibre reinforced concrete in bending. *International Journal of Cement Composites and Lightweight Concrete*, 5(4), pp.225–233.

Nam, J.S. et al., 2011. Evaluation on the Blast Resistance of Fiber Reinforced Concrete. *Advanced Materials Research*, 311-313, pp.1588–1593.

Neville, A. & Aïtcin, P.-C., 1998. High performance concrete—An overview. *Materials and Structures*, 31(2), pp.111–117. Available at: http://www.springerlink.com/index/10.1007/BF02486473 [Accessed April 1, 2014].

Ohtsu, M. et al., 2007. Dynamics of spall failure in fiber reinforced concrete due to blasting. *Construction and Building Materials*, 21(3), pp.511–518.

Paskova, T. & Meyer, C., 1997. Low-cycle fatigue of plain and fiber-reinforced

concrete. *ACI Mater J*, 94(4), pp.273–285.

Petkovic, G., 1991. *Properties of concrete related to fatigue damage with emphasis in high strength concrete*. Univeristetet i Trondheim, Norges tekniske hogskole.

Tabatabaei, Z.S. et al., 2013. Experimental and numerical analyses of long carbon fiber reinforced concrete panels exposed to blast loading. *International Journal of Impact Engineering*, 57, pp.70–80.

Wang, N., Mindess, S. & Ko, K., 1996. Fibre reinforced concrete beams under impact loading. *Cement and Concrete Research*, 26(3), pp.363–376.

Wang, S., Zhang, M.-H. & Quek, S.T., 2012. Mechanical behavior of fiber-reinforced high-strength concrete subjected to high strain-rate compressive loading. *Construction and Building Materials*, 31, pp.1–11.

Wang, Z.L., Konietzky, H. & Huang, R.Y., 2009. Elastic–plastic-hydrodynamic analysis of crater blasting in steel fiber reinforced concrete. *Theoretical and Applied Fracture Mechanics*, 52(2), pp.111–116.

Wang, Z.L., Liu, Y.-S. & Shen, R.F., 2008. Stress–strain relationship of steel fiber-reinforced concrete under dynamic compression. *Construction and Building Materials*, 22(5), pp.811–819.

Wang, Z.L., Wu, J. & Wang, J.G., 2010. Experimental and numerical analysis on effect of fibre aspect ratio on mechanical properties of SRFC. *Construction and Building Materials*, 24(4), pp.559–565.

Wang, Z.L., Wu, L.P. & Wang, J.G., 2010. A study of constitutive relation and dynamic failure for SFRC in compression. *Construction and Building Materials*, 24(8), pp.1358–1363.

Xu, Z., Hao, H. & Li, H.N., 2012a. Dynamic tensile behaviour of fibre reinforced concrete with spiral fibres. *Materials & Design*, 42, pp.72–88.

Xu, Z., Hao, H. & Li, H.N., 2012b. Experimental study of dynamic compressive properties of fibre reinforced concrete material with different fibres. *Materials & Design*, 33, pp.42–55.

Yamaguchi, M. et al., 2011. Blast Resistance of Polyethylene Fiber Reinforced Concrete to Contact Detonation. *Journal of Advanced Concrete Technology*, 9(1), pp.63–71.

Zia, P., Ahmad, S. & Leming, M., 1997. *HIGH-PERFORMANCE CONCRETES: A STATE-OF-ART REPORT*, Available at: http://trid.trb.org/view.aspx?id=725763 [Accessed April 1, 2014].